

Journal of Materials Chemistry C

Accepted Manuscript



This article can be cited before page numbers have been issued, to do this please use: Z. Lu, S. Yang, X. Liu, Y. Qin, S. Lu, Y. Liu, R. Zhao, L. Zheng and H. Zhang, *J. Mater. Chem. C*, 2019, DOI: 10.1039/C9TC00446G.



This is an Accepted Manuscript, which has been through the Royal Society of Chemistry peer review process and has been accepted for publication.

Accepted Manuscripts are published online shortly after acceptance, before technical editing, formatting and proof reading. Using this free service, authors can make their results available to the community, in citable form, before we publish the edited article. We will replace this Accepted Manuscript with the edited and formatted Advance Article as soon as it is available.

You can find more information about Accepted Manuscripts in the [author guidelines](#).

Please note that technical editing may introduce minor changes to the text and/or graphics, which may alter content. The journal's standard [Terms & Conditions](#) and the ethical guidelines, outlined in our [author and reviewer resource centre](#), still apply. In no event shall the Royal Society of Chemistry be held responsible for any errors or omissions in this Accepted Manuscript or any consequences arising from the use of any information it contains.



Journal Name

ARTICLE

Facile synthesis and separation of E/Z isomerization of aromatic-substituted tetraphenylethylene for investigating their fluorescent properties via single crystal analysis

Received 00th January 20xx,
Accepted 00th January 20xx

DOI: 10.1039/x0xx00000x

www.rsc.org/

Zhixiang Lu, Shaoxiong Yang, Xiaolan Liu, Yu Qin, Shuhan Lu, Yanxiong Liu, Ruidun Zhao, Liyan Zheng* and Hongbin Zhang *

The intermolecular interactions and molecular packing form of fluorescent molecules have huge impact on their optical properties, especially for AIE molecules. As a class of typical AIE molecule, tetraphenylethylene (TPE) and its derivatives have prominent optical properties; nevertheless, separation of the mixtures of E/Z isomers is a great challenge. Herein, a series of aromatic-substituted TPE derivatives have been synthesized and used to separate the mixtures of E/Z isomers by common column chromatography with high yields, as confirmed by single crystal, mass spectrometry and NMR spectroscopy. The structure-property relationships of these molecules have been systematically investigated by the combination of spectroscopic methods, theoretical calculations and single crystal data analysis. The E/Z isomers exhibited many different fluorescent properties, such as AIE and mechanochromic behavior. Moreover, the position of N on the substituted pyridine ring also has an effect on the molecule stack pattern and the fluorescent properties. Collectively, our findings could not only improve fundamental understanding of the cis/trans isomerization and photophysical properties of TPE derivatives but also provide a good strategy for designing different substituted groups that can produce various functions and have more potential applications.

1. Introduction

Stereochemistry plays a crucial role on the functional materials and life sciences in modern organic chemistry [1-3]. The stereochemistry of double bonds holds great implications for drug discovery and dye development [4-6]. Isomers that have the same molecular formula but different geometrical positions in space can show entirely different properties [7-9]. Drugs with cis and trans isomers have been reported to differ in their pharmacodynamic and pharmacokinetic properties [10-11]. For example, trans-tamoxifen is a potent estrogen receptor antagonist, which is used for the treatment of breast cancer, however, cis-tamoxifen is a full estrogen agonist [12]. The double bonds are also built-in elements of fluorescent dyes whose cis and trans isomers display different optical properties [13-15]. By controlling the cis/trans isomerization under special stimulation, a variety of applications can be achieved [16-18]. As the most classical smart molecules with light responsive cis/trans isomerization, azobenzene and derivatives have been demonstrated for widespread applications such as light-driven molecular logic gates, data recording and storage, and chemical wiring [19-21]. For these attractive properties and important applications, the development of synthesis and separation techniques to obtain pure isomers for elucidating the characteristic properties of cis and trans geometric isomers and

their isomerization are thus not only useful for fundamental studies but also offering a unique opportunity to explore their practical applications.

The intermolecular interactions and packing model were also affected by their stereochemistry, since they have huge impact on their optical properties, especially for AIE molecules [22-26]. It has been revealed that the optical properties can be modulated by varying the molecular interactions, such as π - π stacking, H-/J-aggregation or hydrogen bonding. Another intriguing property of the responsive optical materials was mechanochromic, that is, the emission colors or intensity of materials can change when they suffer from appropriate external force stimulus such as grinding, shearing, pressing, and crushing, which lead to the changes in intermolecular interactions. In general, mechanical forces can change the pristine packing of molecules, including phase transitions from the crystalline state to the amorphous state, or transition from one crystal stage to another, and the change of intermolecular interactions or molecular structures will induce mechanochromic appearance [27-30].

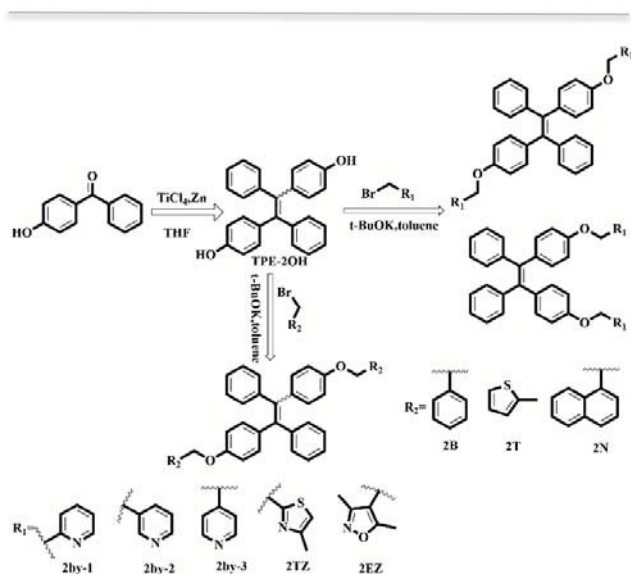
Tetraphenylethylene (TPE) and its derivatives are a class of fluorescent molecules with significant AIE effect, properties with efficient light emission in the aggregate state, which have attracted tremendous researchers to conduct extensive design and application studies [31-35]. Thus far, multiple functional group-substituted TPE derivatives have been applied to bioimaging, biosensing, optoelectronic devices and therapeutic applications [36-40]. Furthermore, the design and synthesis based on TPE and its derivatives with mechanochromic property have become other a hot research field in recent years [41-43]. Rajneesh Misra group reported that TPE substituted pennanthroimidazoles was used as a highly effective mechanochromic material, and further to study the positional effect of the TPE unit by altering the position of the phenyl unit on the imidazole [44]. Nowadays, TPE and its derivatives are usually synthesized by the McMurry coupling

Key Laboratory of Medicinal Chemistry for Natural Resource (Yunnan University), Ministry of Education, Functional Molecules Analysis and Biotransformation key laboratory of Universities in Yunnan Province, School of Chemical Science and Technology, Yunnan University, Kunming, Yunnan 650091, China
E-mail: zhengliyan@ynu.edu.cn (L. Zheng), zhanghb@ynu.edu.cn (H. Zhang)
Electronic Supplementary Information (ESI) available: [details of any supplementary information available should be included here]. See DOI: 10.1039/x0xx00000x

ARTICLE

reaction. However, the product is the mixture of cis and trans isomers due to the unsymmetrical coupling reaction [45]. Owing to these difficulties, most articles researched the mixtures of cis and trans isomers, and these mixtures have compromising effect on the functions and performance in various applications [46-47]. However, there are only a few pure cis/trans isomers have been separated and utilized for research. Tang et al. have reported a number of alkoxy-substituted TPE derivatives and demonstrated their morphology-dependent multicolor emissions by different external stimuli in a solid state [48]. Separating the E/Z isomers of TPE is a huge challenge. After the successful separation, the confirmation of cis/trans geometry is another challenging task. They have synthesized TPE-UPy and separated the isomers with high yield by column chromatography, and the structures of (Z) - TPE-UPy and (E) - TPE-UPy are confirmed by 2D COSY and NOESY NMR spectra [49]. Wu et al. synthesized and purified the E/Z isomers of oxetane-substituted TPE derivatives by column chromatography. Their geometries are also confirmed by NOESY and COSY NMR spectroscopy [50]. Single crystal investigation is the most powerful and convincing tool to reveal the structure and packing model of the molecule. However, most of them did not obtain the single crystal structure of the pure E/Z isomers, which led to difficulties in further research for clarifying their structure-property relationships.

Since the AIE effect and stimuli-responsive property have significantly changed on account that intermolecular interactions and cis/trans isomerization (E/Z isomerization) have different arrangement in space, the AIE phenomenon and stimuli-responsive property of E/Z isomerization are obviously different due to the intermolecular interaction. In addition, the substituted groups have great influence on the intermolecular interaction, resulting in a large change in the optical properties. The E/Z isomerization and different substituted groups are very important to optical properties study of fluorescent materials, and also provide a new strategy for expanding their research. Therefore, it is particularly important and urgent to synthesize and separate the E/Z isomers with a facile method to acquire the accurate structure of pure E/Z isomers, which can be beneficial to investigate structure-property relationships to design functional molecules for various applications on-demand.



Scheme 1. Synthetic route to aromatic-substituted tetraphenylethylene.

Here, a series of TPE derivatives with aromatic-substituted small-groups were designed and synthesized by introducing high polar substituents (pyridine, thiazole, oxazole) and smaller polar substituents (benzene, naphthalene, thiophene), respectively. Moreover, the compound which was introduced with high polar

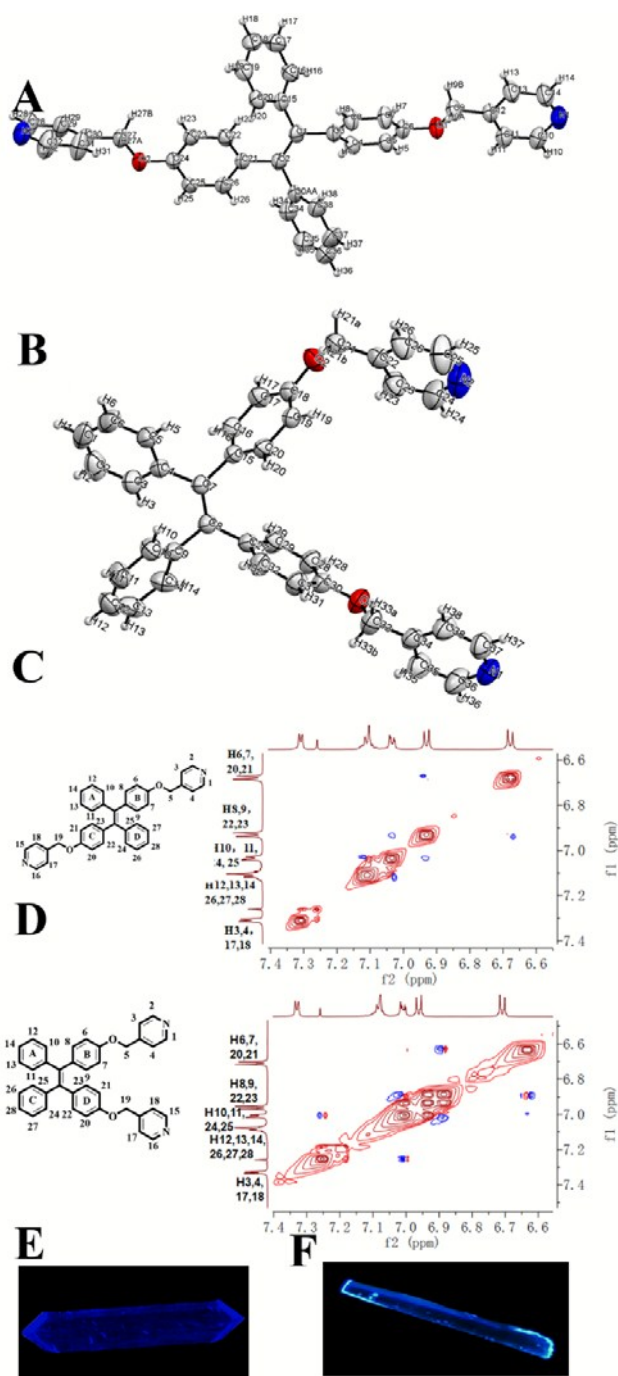


Fig. 1 Crystal structures of TPE-2by-3-E (A) and TPE-2by-3-Z (B). NOESY-NMR of TPE-2by-3-E (C) and TPE-2by-3-Z (D) (enlarged). Single crystal fluorescence pictures of TPE-2by-3-E (E) and TPE-2by-3-Z (F) under the fluorescent inverted microscope.

substituents can be more efficiently separated and purified to obtain the pure E/Z isomers by macro chromatography. It is gratifying to note that each pure E/Z isomers can obtain a single crystal structure, which is confirmed by single crystal measurement, 2D COSY and NOESY NMR spectroscopy. The structure-property relationships of these molecules have been systematically investigated with the combination of spectroscopic methods, theoretical calculations and single crystal data analysis. These results revealed that both E/Z configurations and the position of N on the substituted pyridine ring have an important effect on the molecular packing form, fluorescent property of AIE and mechanochromism activity.

2. Results and discussion

2.1 Design, synthesis and characterization of all compounds.

Although most of the synthetic TPE derivatives by McMurry coupling are highly efficient and versatile, the reaction products are usually the mixture of E/Z isomerization. Based on the similarity in the molecular structure and the polarities of the steric conformation, TPE that links the high polar groups to the periphery may produce sufficient quadratic properties in the structure and polarity which contribute to achieving the macroscopic separation of their stereoisomers. To this point, we designed the structure of the functionalized TPE molecule and achieved its preparation via the synthetic route as shown in Scheme 1. A mixture of 1,2-bis(4-hydroxyphenyl)-1,2-diphenylethylene (TPE-2OH) E/Z stereoisomers were prepared by McMurry coupling. In the next step, E/Z isomerization were synthesized by the one-pot method with nucleophilic substitution reaction between hydroxyl and bromine. We have found that when high polar groups such as pyridine, thiazole and oxazole were introduced, two dots were observed on silica gel plate and the products could be easily separated by common column chromatography. Interestingly, high mass spectrometry showed that the molecular weights of the two new compounds were the same as the one of target molecule, which obviously proves the presence of E/Z isomerization (Fig. S6,9,12,15,18,21,24,27 and 30). However, when the low polar benzene, thiazole, or naphthalene were introduced to the periphery of TPE, only one dot was observed on silica gel plate, indicating the E/Z isomerization mixture could not be separated by common column chromatography.

The E/Z isomers of the two new compounds cannot be distinguished according to ^1H NMR spectroscopy, ^{13}C NMR spectroscopy and FTIR spectroscopy of TPE-2by-1, TPE-2by-2, TPE-2by-3, TPE-2TZ and TPE-2EZ (Fig. S4-33 and Fig. S43). Fortunately, all single crystals of the E/Z isomers are able to be obtained by the solvent diffusion method. The monomer (10 mg) was separated and purified by column chromatography and was dissolved in dichloromethane (0.3 mL), and then the mixture of petroleum ether and ethyl acetate (3:1 = 2.4 mL) were slowly added, and the corresponding single crystal could be obtained after 2-3 days of static storage. The detailed single crystal data were shown in Table 1, and the specific single crystal structures were as displayed in Fig. 1A, B and Fig. S44, which is a direct, accurate and powerful confirmation of the E/Z isomers. Considering the lack of the structure of TPE derivatives, and E/Z isomers were checked based on single crystal structure measurement, and the obtained single crystal structure of our TPE derivatives E/Z isomers can benefit for the investigation of structure-property relationships. The geometry structures of E/Z isomers were further confirmed by 2D COSY and NOESY NMR spectroscopy, which testified these structures shown in supplementary data.

Taking TPE-2by-3-E isomer as an example, the resonance at $\delta = 5.00$ ppm corresponds to the H5 and H19 protons as a reference

for correction. According to this assignment and the explicit correlations in the NOESY spectrum (Fig. S61), the protons with $\delta = 8.51$ and 8.50 ppm are attributed to H1, H2 and H15, H16, respectively, because of their strong correlation with H3, H4 and H17, H18. These protons signal with $\delta = 7.31$ and 7.30 ppm are attributed to H3, H4 and H17, respectively, because of their strong correlation with H5 and H19. The resonance at $\delta = 6.60$ and 6.61 ppm are assigned to H6, H7, H20, and H21 because of their strong correlation with H5 and H19. The resonance at $\delta = 6.85$ and 6.86 ppm belong to H8, H9, H22, and H23, $\delta = 6.96$ and 6.95 ppm are attributed to H10, H11, H24, and H25, $\delta = 7.12$ and 7.14 ppm are ascribed to H12, H13, H14, and H26, H27, H28, respectively. As shown in Fig. 1C and Fig. S61, the cross-peaks in the blue circles indicate obvious correlations between H10/H11/H24/H25 and H8/H9/H22/H23, which indicates that ring A and ring C are close in space, and means they are on the same side of the double bond. However, there are no correlations for those hydrogens in COSY NMR spectroscopy (Fig. S62–S63). In the meantime, we cannot find clear correlations between H10/H11/H24/H25 and H8/H9/H22/H23 in Fig. 1D; because ring A/C are far from ring B/D in Z isomers (Fig. S64–S66). Consequently, the NOESY and COSY NMR spectroscopy confirmed the geometrical structures of the

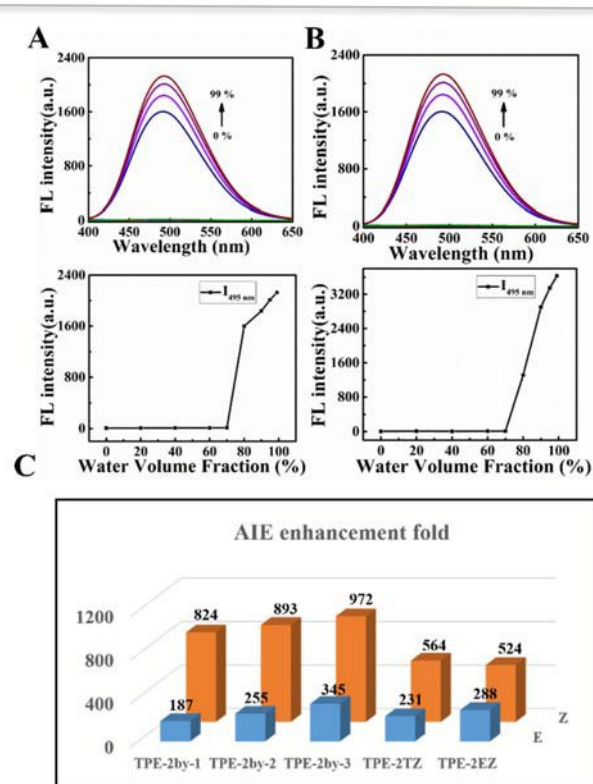


Fig. 2 Fluorescent spectra of TPE-2by-3-E (A) and TPE-2by-3-Z (B) (1×10^{-5} M, $\lambda_{\text{ex}} = 340$ nm) in DMF and water mixtures with different water fractions (below: and plots of fluorescence intensity versus water fractions). (C) AIE enhancement multiple histogram of all Z/E isomers.

Table 1. Selected crystallographic data for compounds.

	TPE-2by-1-E	TPE-2by-1-Z	TPE-2by-2-E	TPE-2by-2-Z	TPE-2by-3-E	TPE-2by-3-Z	TPE-2TZ-E	TPE-2TZ-Z	TPE-2EZ-E	TPE-2EZ-Z
Formula	C ₁₈ H ₁₀ N ₂ O ₂	C ₁₈ H ₁₀ N ₂ O ₂	C ₁₈ H ₁₀ N ₂ O ₂	C ₁₈ H ₁₀ N ₂ O ₂	C ₁₈ H ₁₀ N ₂ O ₂	C ₁₈ H ₁₀ N ₂ O ₂	C ₁₈ H ₁₂ N ₂ O ₂ S ₂	C ₁₈ H ₁₂ N ₂ O ₂ S ₂	C ₁₈ H ₁₄ N ₂ O ₄	C ₁₈ H ₁₄ N ₂ O ₄
<i>f_w</i> [g·mol ⁻¹]	546.64	546.64	546.64	546.64	546.64	546.64	588.76	588.76	582.67	582.67
crystal color	colourless	colourless	colourless	colourless						
crystal system	Triclinic	Monoclinic	Monoclinic	Monoclinic	Monoclinic	Monoclinic	Triclinic	Monoclinic	Monoclinic	Triclinic
space group	P -1	C2/c	P1 21/n 1	C 2/c	P 21/c	P1 21/n 1	P -1	P1 21/n 1	P2(1)/n	P -1
<i>a</i> [Å]	9.750(2)	17.97(3)	9.72023(14)	17.704(19)	14.386(7)	22.5985(5)	11.174(3)	18.3912(4)	12.0607(18)	10.741(5)
<i>b</i> [Å]	11.263(3)	10.134(15)	9.20409(15)	10.131(11)	11.778(11)	5.88283(9)	12.359(4)	16.5233(3)	10.4171(15)	12.302(6)
<i>c</i> [Å]	13.618(3)	18.39(3)	32.4449(4)	18.53(3)	19.177(14)	23.3075(5)	13.771(4)	10.1810(2)	26.268(4)	13.583(6)
<i>β</i> [deg]	92.030(3)	116.463(12)	97.3047(13)	117.784(13)	98.760(9)	108.792(2)	80.595(4)	97.1241(19)	101.731(2)	112.723(6)
<i>V</i> [Å ³]	1478.0(6)	2997(8)	2879.15(7)	2940(6)	3212(4)	2933.40(11)	1777.7(9)	3069.95(11)	3231.4(8)	1599.5(13)
<i>Z</i>	2	8	4	8	4	4	2	4	4	2
<i>ρ</i> _{calc} [g/cm ³]	1.228	1.212	1.261	1.235	1.197	1.238	1.319	1.274	1.198	1.210
<i>μ</i> [mm ⁻¹]	0.076	0.075	0.610	0.076	0.076	0.599	0.410	1.844	0.078	0.078
<i>T</i> [K]	293(2)	293(2) K	298(2) K	293(2) K	298(2) K	298 K	293(2) K	298 K	298(2) K	298(2) K
<i>θ</i> _{min} – <i>θ</i> _{max} [deg]	2.092–25.000	2.375–24.996	0.959–74.192	2.394–25.148	2.036–24.995	0.965–74.200	1.543–25.149	0.974–74.070	1.745–24.997	1.674–25.149
<i>R</i> / <i>wR</i> [<i>I</i> > 2 <i>σ</i> _{<i>I</i>}]	0.0511/0.1308	0.0511/0.1557	0.0564/0.1487	0.0460/0.1124	0.0544/0.1096	0.0494/0.1562	0.0758–0.2010	0.0713/0.2241	0.0575/0.1328	0.0630/0.1527

E/Z isomers of TPE-2by-3 molecule. This result is consistent with the single crystal structure. The geometry structures of other molecules (TPE-2by-1-E, TPE-2by-1-Z, TPE-2by-2-E, TPE-2by-2-Z, TPE-2TZ-E, TPE-2TZ-Z, TPE-2EZ-E, TPE-2EZ-Z) were confirmed by the NOESY and COSY NMR spectroscopy, which were similar with TPE-2by-3-E and TPE-2by-3-Z, mainly from the correlation of hydrogen on the TPE benzene ring. The detailed information about their NOESY and COSY NMR spectroscopy data were shown as in Fig. S45–S82. These results of all E/Z isomers are consistent with the single crystal structures (Fig. S44). Crystallographic data for compounds as shown in Table 1. All the single crystal data were submitted to the Cambridge Crystallographic Data Centre (CCDC), and each compound has its corresponding number, 1833475 (TPE-2by-1-E), 1833476(TPE-2by-1-Z), 1833477(TPE-2by-2-E), 1833478(TPE-2by-2-Z),1833479(TPE-2by-3-E), 1833480(TPE-2by-3-Z), 1833481(TPE-2TZ-E), 1833482(TPE-2TZ-Z), 1833483(TPE-2EZ-E) and 1833484(TPE-2EZ-Z). All single crystals displayed strong blue fluorescence through the fluorescent inverted microscope, as displayed in Fig. 1E/F and Fig. S83.

2.2 Photophysical properties in solution.

After the structure confirmation, the AIE properties of all compounds were investigated to verify that these TPE derivatives

are a series of typical AIE molecules. As can be seen from Fig. 2 and Fig. S84, all compounds exhibit good solubility in N, N-Dimethylformamide (DMF), but they are insoluble in water due to the hydrophobic aromatic rings. Fluorescence spectra of the luminogens in DMF and DMF/H₂O mixtures were measured. TPE-2by-3-E in pure DMF and DMF/H₂O mixtures with water fractions (*f_w*) lower than 80 % have no emission, which is as a result of the active intermolecular rotations of the dissolved luminogens in these mixtures. The fluorescence intensity starts to increase when (*f_w*) is larger than 80 %, at which the compound begins to aggregate. When *f_w* was up to 99 %, its fluorescence intensity is 345-fold higher than that in pure DMF (Fig. 2A) at 500 nm, thus certifying its AIE behaviour. Other molecules show similar AIE behaviour compared to TPE-2by-3-E. The fluorescence enhancement of TPE-2by-3-Z at *f_w* = 99 % was 972 times stronger than that in pure DMF (Fig. 2B). As shown in Fig. S84 and Fig. 2C, there are two interesting phenomena that are worth noting according to the enhancement multiplier of these E/Z isomerization. Firstly, Z isomerization has more significant AIE enhancement than the E isomerization under the same conditions. Secondly, there is a significant difference in AIE effect among the molecular whose position of N atom is different in pyridine substituents. For the pyridine group of E isomerization, the AIE enhancement fold was increased with an order of ortho-position, meta-position and para-position, and the Z isomerization is also following the same tendency. These results indicated both E/Z isomerization and the position of N atom in pyridine have important effect on the AIE behaviour of these TPE derivatives.

2.3 Mechanochromism property.

The controllable discoloration behaviour of organic materials, including some TPE derivatives have attracted much attention due to their potential applications in sensors, memories, logic gate units, security inks, etc [30-38]. However, the fluorescent color of TPE-2OH did not change after grinding, suggesting this molecule didn't display mechanochromism property. Interestingly, after introducing substituted group into TPE-2OH, all the compounds showed a characteristic color variation upon grinding, suggesting the importance of introducing substituted group for mechanochromism. In other words, introducing substituent is an efficient and facile strategy for developing mechanochromism materials. To evaluate the mechanochromism behaviour of all compounds, their solid-state emissions were investigated. As shown in Fig. 3, the as-prepared solid powder of TPE-2by-3-E has an intense blue fluorescence in pristine state, and the fluorescence turns to bright green after grinding, and then the fluorescence quickly turns back to its original blue fluorescence after being fumed by DCM vapor. The change of fluorescent color can be distinctly distinguished by naked eye under UV light. Other TPE derivatives demonstrated the similar phenomenon with TPE-2by-3-E when they were subjected to grinding stimulation and fumed by DCM vapor.

The mechanochromic properties of these aromatic-substituted tetraphenylethylene were studied by emission and absorption spectrum in detail. The emission spectra of all compounds under external grinding were shown in Fig. 4 A/B and Fig. S85, and the solid UV absorption of all compounds under external grinding were shown in Fig. 4 C/D and Fig. S87. In addition, the corresponding spectroscopic data were summarized in Table 2 and Table S1-7. The TPE-2by-3-E isomers at the pristine state emits at 449 nm, which display red-shifted emission peak upon grinding at 489 nm. It can return back to the original state after being fumed by DCM vapor. At the same time, the fluorescence red-shifted of TPE-2by-3-Z isomers solid from 440 nm to 496 nm. Under the same conditions, we discovered that the red-shifted of TPE-2by-3-Z ($\Delta\lambda$ 56 nm) was greater than that of TPE-2by-3-E ($\Delta\lambda$ 40 nm) after grinding. The fluorescence spectra of other compounds in the pristine state and after grinding are shown in Fig. S86, and the red-shifted emission ($\Delta\lambda$) is presented in Table S1-7. These results revealed that the solid powder samples of Z isomers exhibit a larger red-shifted in emission comparing with the one of E isomers, and that the red-shifted of para-position N atm in pyridine substituents are larger than those of meta -position and ortho -position of E and Z isomers.

Obvious change in the UV/vis absorption band was observed before and after grinding the powder as shown in Fig. 4C/D and Fig. S87. The UV/vis absorption band changes of all compounds are almost the same. UV/vis absorption also has a significant red-shifted after grinding, and strong new absorption peaks are generated at 270 nm and 330 nm. These absorption peaks could be ascribed to $n \rightarrow \pi^*$ transition. The red-shift of the absorption

Fig. 3 Fluorescent images of TPE-2by-3-E (A) and TPE-2by-3-Z (B) in different treatments: 1. Pristine; 2. Grinding at one side; 3. Grinding all; 4. Fumed by DCM.

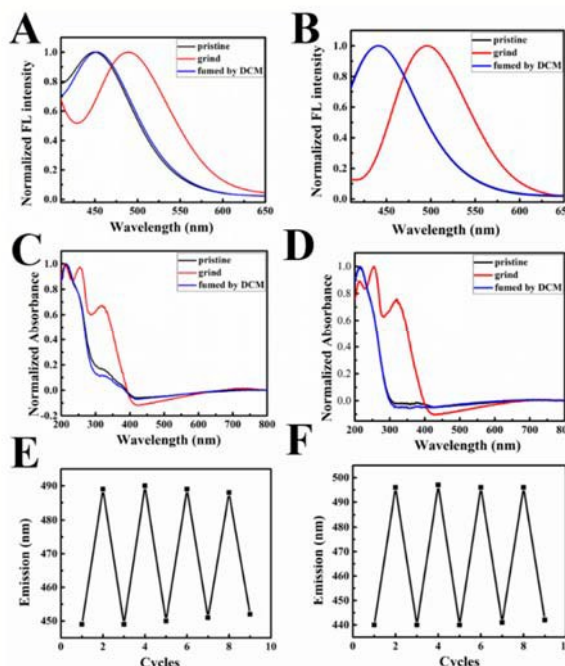


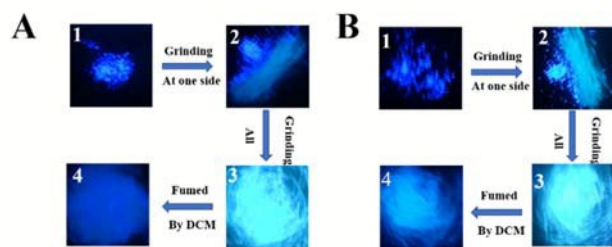
Fig. 4 Fluorescent spectra of TPE-2by-3-E (A) and TPE-2by-3-Z (B): pristine, ground, and fumed by DCM. Solid UV absorption of TPE-2by-3-E (C) and TPE-2by-3-Z (D): pristine, ground, and fumed by DCM. Reversible switching of emission of TPE-2by-3-E (E) and TPE-2by-3-Z (F) by repeated grinding- fuming by DCM.

Table 2. Spectroscopic data for TPE-2by-3-E and TPE-2by-3-Z.

Name	treatment	E_m (nm)	$\Delta\lambda$ (nm)	Φ_f (%)	τ (ns)	$k_f/10^8$ (s ⁻¹)	$k_{nr}/10^8$ (s ⁻¹)	ΔE (KJ/mol)
TPE-2by-3-E	pristine	449	40	27.4	3.07	0.89	2.36	380.75
	grind	489		44.2	4.29	1.03	1.30	
	fumed by DCM	451	26.8	3.07	0.87	2.31		
TPE-2by-3-Z	pristine	440	56	33	3.14	1.04	2.15	382.19
	grind	496		45.5	4.35	1.05	1.25	
	fumed by DCM	441	32.8	3.14	1.03	2.16		

and fluorescence spectra after grinding may originate from the increased molecular interaction with decreasing the optical bandgap of the molecules in the ground sample. As shown in Fig. 4E/F, the blue-green emission color change is reversible and recyclable for several cycles when TPE-2by-3-E and TPE-2by-3-Z repeat grinding- fuming by DCM process.

To better explain the different spectroscopic properties between the luminogens, we further analysed their structure by powder X-ray diffraction (XRD) measurement. The XRD patterns revealed that as-prepared TPE-2by-3-E isomers powder features a series of sharp diffraction peaks. Upon grinding, the crystalline structure almost completely converts to amorphous phase as indicated from the XRD patterns, as can be seen in Fig. 5A. The change in crystal form of TPE-2by-3-Z in Fig. 5B is also a transition from crystalline to amorphous. Detailed XRD changes of other molecules are shown in Fig. S90. There is a significant difference between the XRD of the E and Z isomers, but both of them are transformed into amorphous after grinding. The ground sample will promptly re-crystallize when the sample was fumed by DCM



ARTICLE

Journal Name

vapor treatment as can be seen in the regain of intensity and peaks in XRD patterns. Clearly, the reversible transition between the ordered crystalline state and amorphous state is vital to the switchable emission color and intensity of the luminophor. Similar properties were observed in other TPE derivatives.

In order to understand more details about the characteristic optical properties of all aromatic-substituted tetraphenylethylene solid, fluorescence quantum yield (Φ) and fluorescence lifetime (τ) of these compounds were measured. The fluorescence quantum yield and fluorescence lifetime of TPE-2by-3-E in crystal state are 27.4 % and 3.07 ns, TPE-2by-3-Z are 33 % and 3.14 ns, respectively. The fluorescence radiative rate constant (k_r) and non-radiative rate constant (k_{nr}) were estimated by combining the quantum yield [$\Phi = k_r / (k_r + k_{nr})$] and fluorescence lifetime results [$\tau = (k_r + k_{nr})^{-1}$]. According to the formula, the fluorescence radiative rate constant is calculated to be $0.89 \times 10^8 \text{ s}^{-1}$ and non-radiative rate constant is calculated to be $2.36 \times 10^8 \text{ s}^{-1}$ of TPE-2by-3-E isomers in the pristine state. However, the fluorescence radiative rate constant of TPE-2by-3-Z isomers is $1.04 \times 10^8 \text{ s}^{-1}$, which is higher than that of TPE-2by-3-E isomers. The non-radiative rate constant of TPE-2by-3-Z isomers is $2.15 \times 10^8 \text{ s}^{-1}$, which is lower than that of TPE-2by-3-E isomers. This suggests that molecular packing of the Z isomers may effectively inhibits the excited energy loss through a non-radiative decay process.

After being subjected to grinding stimuli, the fluorescence quantum yield, fluorescence lifetime of TPE-2by-3-E and TPE-2by-3-Z are all increased, and the non-radiative rate constant is reduced, as shown in Table 2. The variations of other molecule properties are the same as that of TPE-2by-3-E, and all the data are summarized in Table S1-S7 and Fig. S88. The decrease of k_{nr} is remarkable while the change of k_r is not obvious after grinding, indicating that the decreasing non-radiative decay process effectively suppresses energy loss and benefit for the fluorescent emission. In the pristine state, the fluorescence quantum yield, fluorescence lifetime of all Z isomers are larger than that of E isomers, and the non-radiative rate constant are smaller. In view of the TPE derivatives of the pyridine substituents in the E isomers, the fluorescence quantum yields, fluorescence lifetimes of the ortho, para, and meta positions are gradually increasing, and the fluorescence non-radiative rate constant is gradually reducing, and the same tendency for the Z isomers is observed. The fluorescence non-radiative rate constants of TPE-2by-3 decrease more prominently, indicating that the non-radiative delay process is inhibited, as shown in Fig. S89.

2.4 Theoretical study.

To obtain a better understanding of the optical properties of all E/Z isomerization, we carried out theoretical calculations on their energy levels by the density functional theory (DET) method at B3LYP/6-31G(d) basis in the Gaussian 09. The simulation results including optimized molecular configuration, energy levels and electron distribution of the high occupied molecular orbital (HOMO) and lowest unoccupied molecular orbital (LUMO) of TPE-2by-3-E and TPE-2by-3-Z are shown in Fig. 6A/B. And the calculation of other E/Z isomers are displayed in Fig. S91. According to our theoretical calculation results, the calculated

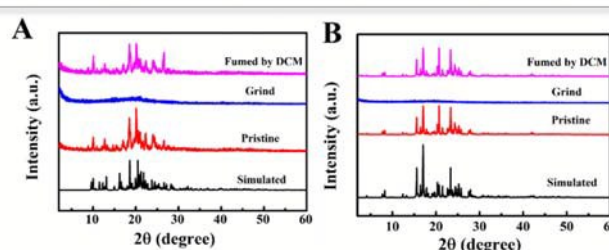


Fig. 5 XRD patterns of TPE-2by-3-E (A), TPE-2by-3-Z (B) pristine, ground, and fumed by DCM.

HOMO and LUMO of the E and Z isomers are almost the same, suggesting the substituent groups have no much effect on the energy levels and electron distribution of these molecules. Here, we employ the TPE-2by-3-E and TPE-2by-3-Z as representatives. For TPE-2by-3-E and TPE-2by-3-Z, the electron intensity of the LUMO is mainly distributed over the benzene ring of TPE, whereas the HOMO is distributed in the double bond. The LUMO-HOMO gap for all E/Z isomers as shown in Fig. 6A/B and Fig. S91. The energy gap of the Z isomers is comparable to the one of E isomers, such as, TPE-2by-3-E is 380.57 KJ/mol, TPE-2by-3-Z is 382.19 KJ/mol in the Table 2. Other detailed data comparisons were shown in supporting information table S1-7. In addition, for pyridine-substituted TPE, and the energy gaps of E and Z isomers of the ortho, meta and para positions are gradually increasing.

2.5 Single crystal structure analysis.

Since the importance of molecule packing forming on the AIE and mechanochromism behaviour, we analysed their single crystal structures to investigate structure-property relationships. As illustrated in Fig. 1A/B and Fig. S44, all molecules adopt a highly twisted conformation. TPE-2by-1-E belongs to triclinic system in p-1 space group while TPE-2by-1-Z is monoclinic system in C 2/c space group. TPE-2by-2-E and TPE-2by-2-Z are monoclinic system in P1 21/n 1, C 2/c space group, respectively. TPE-2by-3-E and TPE-2by-3-Z belong to monoclinic system in P 21/c, P1 21/n 1 space group, respectively. TPE-2TZ-E is triclinic system in p-1 space group, but TPE-2TZ-Z belongs to monoclinic system in P1 21/n 1 space group, TPE-2EZ-E belongs to monoclinic system in P2(1)/n space group, and TPE-2EZ-Z is triclinic system in p-1 space group. Their packing structures of single crystal are shown in Fig. 6C/D and Fig. S92. Van de Waals forces, numerous intermolecular C-H \cdots π (phenyl ring), C-H \cdots H-C and C-H \cdots N (hydrogen bond) contacts, and even local π - π interactions are observed in the crystals. The length of C-H \cdots N hydrogen bond of these TPE derivatives were summarized in Fig. 7. The C-H \cdots N interaction distance of these TPE derivatives are between 2.5 and 3.4 Å. The result indicated all of them are smaller than 3.4 Å, revealing the presence of C-H \cdots N hydrogen bond. The corresponding C-H \cdots N hydrogen bond interaction distance of TPE-2by-3-E is 3.0990 Å, which is a much weaker than TPE-2by-3-Z (2.5852 Å), indicating that the C-H \cdots N interaction in TPE-2by-3-Z is stronger

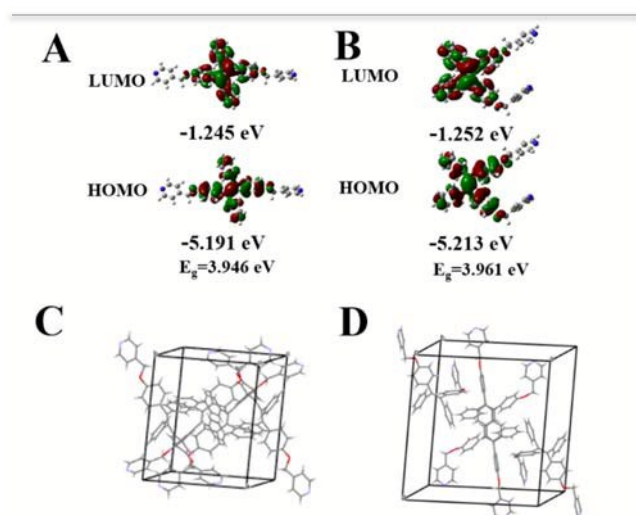


Fig. 6 Energy levels of LUMO and HOMO, energy gaps, and electron cloud distributions of TPE-2by-3-E (A) and TPE-2by-3-Z (B). Packing structure of single crystal about TPE-2by-3-E (C) and TPE-2by-3-Z (D).

than TPE-2by-3-E. Impressively, C–H \cdots N interaction of the Z isomers is stronger than the E isomers as shown in Fig. 7C. In the meantime, C–H \cdots π (phenyl ring) is discovered between the H atom on the labelled phenyl ring and the center of the labelled phenyl, and the distances are also summarized in Fig. 7D. The C–H \cdots π interaction distance of these TPE derivatives are among 3.0 to 3.6 Å, indicating the presence of C–H \cdots π interaction in them. However, the difference in C–H \cdots π interaction distance was much smaller than C–H \cdots N interaction among E/Z isomers. For example, the C–H \cdots π interaction distance of TPE-2by-3-E and TPE-2by-3-Z are 3.0541 Å and 3.0087 Å, respectively.

According to the above structure analyses, the relationship between the optical properties of the TPE derivatives E/Z isomers and their structure can be established. The difference in optical properties of the E/Z isomers molecules is mainly ascribed to the C–H \cdots N hydrogen bond interaction between molecules. The Z isomers have stronger hydrogen bonding force than E isomers, in which the intramolecular rotations are greatly hampered inducing the excited energy loss through a non-radiative decay process and resulting in Z isomers have more significant AIE effect, stronger fluorescence lifetime, higher fluorescence quantum yield, and larger mechanochromic induced wavelength shift than isomers. Typically, the presence of the strongest C–H \cdots N interaction in TPE-2by-3-Z among these TPE derivatives endowed them with the most outstanding AIE and mechanochromic property. As previous mentioned, Z isomers exhibit a greater red-shifted in emission than the one of the E isomers. Based on the crystal analysis, the C–H \cdots π interaction of Z isomers is comparative to the one of E isomers while C–H \cdots N interaction is stronger, resulting in Z isomers exhibit a greater red-shifted in emission than the one of the E isomers. The synergetic effect between the intermolecular interactions (C–H \cdots N interaction) and molecular packing (C–H \cdots π interaction) induced the red-shifted of para-position N atom in pyridine substituents is larger than those of meta -position and ortho -position of E and Z isomers.

3. Conclusions

In this work, we have successfully synthesized a series of aromatic-substituted tetraphenylethylene derivatives through reasonable structure design, and separated their pure isomerization by the common column chromatography technique

and obtained single crystals of all cis/trans isomers. The availability of pure stereoisomers and single crystal data enable us to clearly reveal the relationship between chemical structure and photophysical properties. Interestingly, the Z isomerization have more significant AIE enhancement than the E isomerization under the same conditions. Moreover, there is a significant difference in AIE effect among the isomers with different position of N atom in pyridine substituents. In the solid state, the Z isomers show bathochromic emission with a higher quantum yield and long lifetime compared with the E isomers. After the solid powder was grounded, both the fluorescence quantum yield and fluorescence lifetime increased, and the non-radiative rate constant decreased compared to the one of original state powder. The E/Z isomers display different mechanochromic behaviour as they exhibit reversible and recyclable blue-green emission color switch for several circles gets through repeated grinding- fuming by DCM process. Thanks to the unique mechanochromic property of TPE, it will have great potential applications in stimuli-responsive materials. Single crystal data analysis revealed that all E/Z isomers have strong hydrogen bond and the C–H \cdots N interaction, which of the Z isomers is stronger than the one of E

isomers. The C–H \cdots N hydrogen bond interaction played an important role in the fluorescent properties, including AIE behaviour and mechanochromic performance. Finally, these consequences promote us to understand the relationship

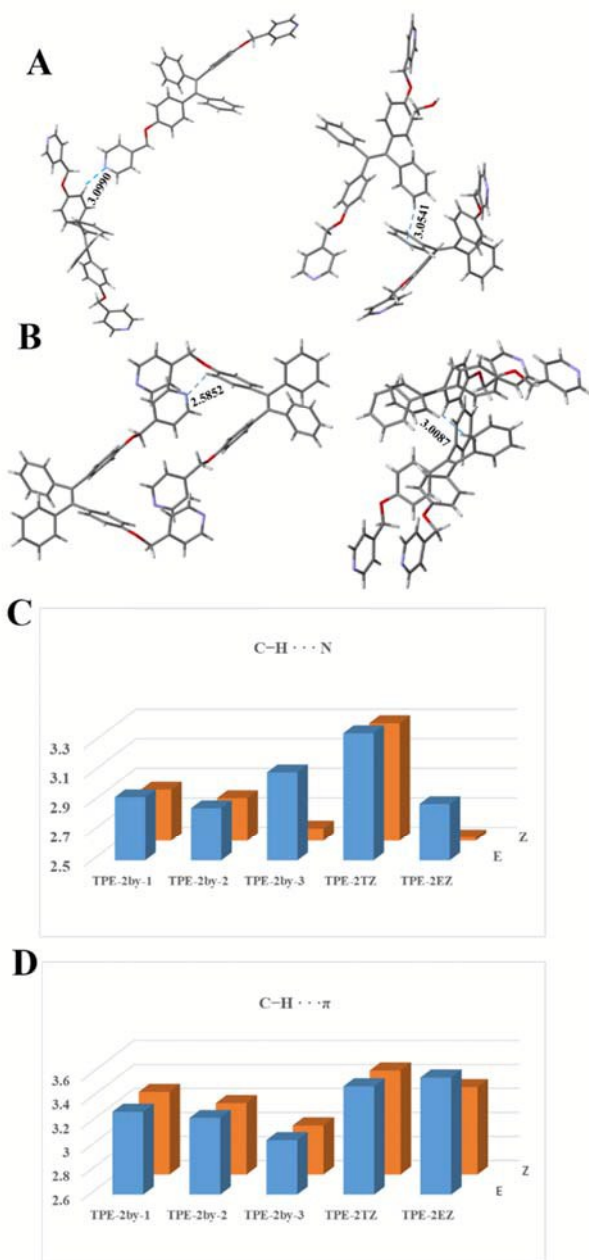


Fig. 7 Intermolecular interactions of TPE-2by-3-E (A) and TPE-2by-3-Z (B). The histogram of C-H...N interaction (C) and (D).

between structures and properties of these TPE derivative E/Z isomers, which are beneficial to the design and synthesis of functional TPE derivatives for various applications.

4. Conflicts of interest

There are no conflicts to declare.

5. Acknowledgements

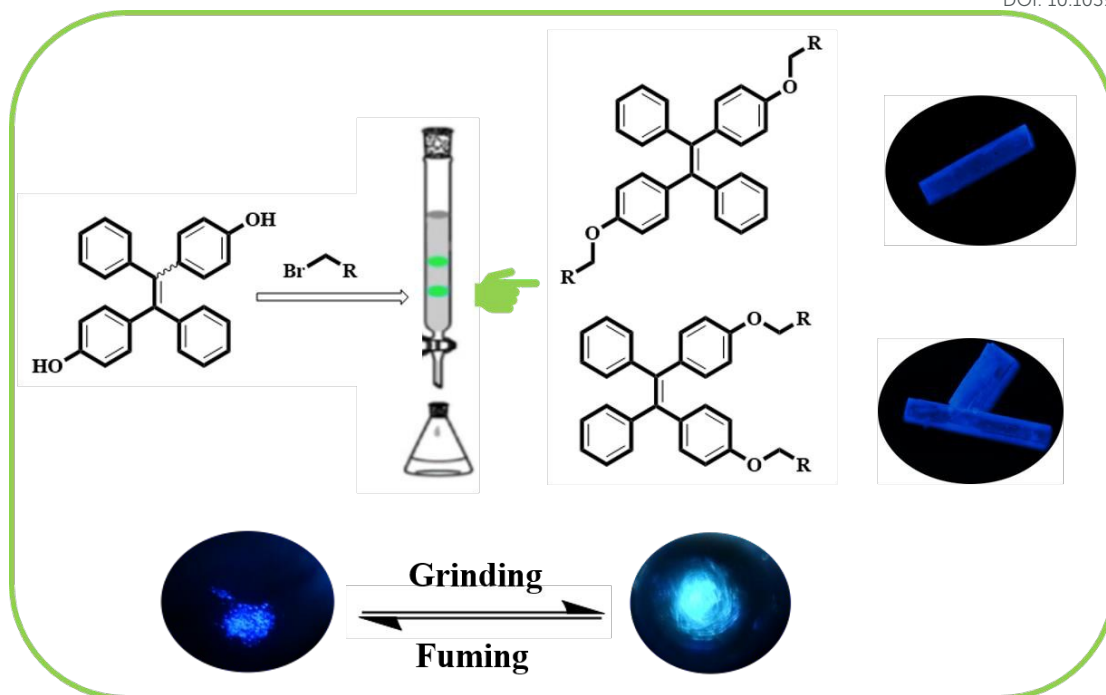
This work was financially supported by the National Natural Science Foundation of China (NSFC, 21765024) and program for

changjiang scholars and innovative research team in university (IRT_17R94)

6. Notes and references

- 1 S. J. Danishefsky, E. Larson, D. Askin and N. Kato, *J. Am. Chem. Soc.*, 1985, **107**, 1247.
- 2 M. C. Fournié-Zaluski, E. Lucas-Soroça, J. Devin and B. P. Roques, *J. Med. Chem.*, 1986, **29**, 751-75.
- 3 P. Palladino, *Isis*, 1990, **81**, 44-67.
- 4 P. S. Watson, B. Jiang and B. Scott, *Org. Lett.*, 2000, **2**, 3679-3681.
- 5 E. M. Driggers, S. P. Hale, J. B. Lee and N. K. Terrett, *Nat. Rev. Drug Discov.*, 2008, **7**, 608.
- 6 O. McConnell, A. Bachli, C. Balibar, N. Byrne, Y. X. Cai, G. Carter, M. Chlenov, L. Di, K. Fan, I. Goljer, Y. N. He, D. Herold, M. Kagan, E. Kerns, F. Koehn, C. Kraml, V. Marathias, B. Marquez, L. McDonald, L. Nogle, C. Petucci, G. Schlingmann, G. Tawa, M. Tischler, R. Thomas, W. Sutherland, W. Watts, M. Young, M. Y. Zhang, Y. R. Zhang, D. H. Zhou and D. Ho, *Chirality: The Pharmacological, Biological, and Chemical Consequences of Molecular Asymmetry*, 2007, **19**, 658-682.
- 7 J. W. Chung, S. J. Yoon, B. K. An and S. Y. Park, *J. Phys. Chem. C.*, 2013, **117**, 11285-11291.
- 8 M. J. K. Harper, A. L. Walpole. *Nature*, 1966, **212**, 87.
- 9 A. Boëdec, H. Sicard, J. Dessolin, I. G. Herbertte, S. Ingoure, C. Raymond, C. Belmont and J. L. Kraus, *J. Med. Chem.*, 2008, **51**, 1747-1754.
- 10 L. E. P. Santiago, C. García, V. L. Vallet, M. A. Miranda and R. Oyola, *Photochem. Photobiol.*, 2011, **87**, 611-617.
- 11 N. Chhabra, M. L. Aseri and D. Padmanabhan, *International journal of applied and basic medical research*, 2013, **3**, 16.
- 12 M. L. Williams, M. S. Lennard, I. J. Martin and G. T. Tucker, *Carcinogenesis*, 1994, **15**, 2733-2738.
- 13 K. J. Smit and K. P. Ghigginoto, *Dyes and pigments*, 1987, **8**, 83-97.
- 14 G. Boice, B. O. Patrick, R. McDonald, C. Bohne and R Hicks, *J. Org. Chem.*, 2014, **79**, 9196-9205.
- 15 R. Y. Tsien, *Angew. Chem.*, 2009, **121**, 5721-5736.
- 16 C. J. Zhang, G. X. Feng, S. D. Xu, Z. S. Zhu, X. M. Lu, J. Wu and B. Liu, *Angew. Chem. Int. Ed.*, 2016, **55**, 6192-6196.
- 17 G. Fischer, T. Tradler and T. Zarnt, *FEBS letters*, 1998, **426**, 17-20.
- 18 T. Kobayashi, T. Saito and H. Ohtani, *Nature*, 2001, **414**, 531.
- 19 C. Zhang, M. H. Du, H. P. Cheng, X. G. Zhang, A. E. Roitberg and J. L. Krause, *Phys. Rev. Lett.*, 2004, **92**, 158301.
- 20 B. A. Yu, Bobrovsky, N. I. Boiko, V. P. Shibaev and J. Springer, *Adv. Mater.*, 2000, **12**, 1180-1183.
- 21 Z. F. Liu, K. Hashimoto and A. Fujishima, *Nature*, 1990, **347**, 658.
- 22 J. L. Humphrey, K. M. Lott, M. E. Wright and D. Kuciauskas, *J. Phys. Chem. B.*, 2005, **109**, 21496-21498.
- 23 H. Tong, Y. Q. Dong, Y. N. Hong, M. Häussler, J. W. Y. Lam, H. H. Y. Sung, X. M. Yu, J. X. Sun, I. D. Williams, H. S. Kwok and B. Z. Tang, *J. Phys. Chem. C.*, 2007, **111**, 2287-2294.
- 24 Z. J. Zhao, P. Lu, J. W. Y. Lam, Z. M. Wang, C. Y. K. Chan, H. H. Y. Sung, I. D. Williams, Y. G. Ma and B. Z. Tang, *Chem. Sci.*, 2011, **2**, 672-675.
- 25 F. Bu, R. H. Duan, Y. J. Xie, Y. P. Yi, Q. Peng, R. R. Hu, A. J. Qin, Z. J. Zhao and B. Z. Tang, *Angew. Chem. Int. Ed.*, 2015, **54**, 14492-14497.
- 26 Y. Dong, Z. M. Yang, Z. J. Ren and S. K. Yan, *Polym. Chem.*, 2015, **6**, 7827-7832.
- 27 Y. Q. Dong, J. W. Y. Lam and B. Z. Tang, *J. Phys. Chem. Lett.*, 2015, **6**, 3429-3436.
- 28 X. F. Mei, J. W. Wang, Z. G. Zhou, S. Y. Wu, L. M. Huang, Z. H. Lin and Q. D. Ling, *J. Mater. Chem. C.*, 2017, **5**, 2135-2141.

- 29 H. Y. Tian, P. P. Wang, J. Liu, Y. X. Duan and Y. Q. Dong, *J. Mater. Chem. C.*, 2017, **5**, 12785–12791.
- 30 J. Q. Shi, L. E. Aguilar Suarez, S. J. Yoon, Sh. Varghese, C. Serpa, S. Y. Park, L. Lüer, D. R. Sanjuan, B. M. Medina and J. Gierschner, *J. Phys. Chem. C.*, 2017, **121**, 23166–23183.
- 31 R. Misra, T. Jadhav, B. Dhokale and S. M. Mobin, *Chem. Commun.*, 2014, **50**, 9076–9078.
- 32 Z. J. Zhao, S. M. Chen, X. Y. Shen, F. Mahtab, Y. Yu, P. Lu, J. W. Y. Lam, H. S. Kwoka and B. Z. Tang, *Chem. Commun.*, 2010, **46**, 686–688.
- 33 Z. J. Zhao, P. Lu, J. W. Y. Lam, Z. M. Wang, C. Y. K. Chan, H. H. Y. Sung, I. D. Williams, Y. G. Ma and B. Z. Tang, *Chem. Sci.*, 2011, **2**, 672–675.
- 34 Y. Q. Dong, J. W. Y. Lam, A. J. Qin, J. Z. Liu, Z. Li and B. Z. Tang, *Appl. Phys. Lett.*, 2007, **91**, 011111.
- 35 H. G. Lu, Y. D. Zheng, X. W. Zhao, L. J. Wang, S. Q. Ma, X. Q. Han, B. Xu, W. J. Tian and H. Gao, *Angew. Chem. Int. Ed.*, 2016, **55**, 155–159.
- 36 Y. Y. Huang, G. X. Zhang, F. Hu, Y. L. Jin, R. Zhao and D. Q. Zhang, *Chem. Sci.*, 2016, **7**, 7013–7019.
- 37 V. S. Vyas and R. Rathore, *Chem. Commun.*, 2010, **46**, 1065–1067.
- 38 D. D. La, S. V. Bhosale, L. A. Jones and S. V. Bhosale, *ACS Appl. Mater. Interfaces*, 2018, **10**, 12189–12216.
- 39 K. Han, S. B. Wang, Q. Lei, J. Y. Zhu and X. Z. Zhang, *ACS Nano*, 2015, **9**, 10268–10277.
- 40 Q. S. Li, Z. M. Yang, Z. J. Ren and S. K. Yan, *Macromol. Rapid Commun.*, 2016, **37**, 1772–1777.
- 41 Z. Chen, G. Liu, S. Z. Pu and S. H. Liu, *Dyes and Pigments*, 2018, **159**: 499–505.
- 42 Z. Y. Ma, Z. J. Wang, X. Meng, Z. M. Ma, Z. J. Xu, Y. G. Ma and X. R. Jia, *Angew. Chem. Int. Ed.*, 2016, **55**, 519–522.
- 43 T. Jadhav, J. M. Choi, J. Shinde, J. Y. Lee and R. Misra, *J. Mater. Chem. C.*, 2017, **5**, 6014–6020.
- 44 T. Jadhav, J. M. Choi, B. Dhokale, S. M. Mobin, J. Y. Lee and R. Misra, *J. Phys. Chem. C.*, 2016, **120**, 18487–18495.
- 45 X. F. Duan, J. Zeng, J. W. Lu and Z. B. Zhang, *J. Org. Chem.*, 2006, **71**, 9873–9876.
- 46 J. Y. Niu, J. L. Fan, X. Wang, Y. S. Xiao, X. I. Xie, X. Y. Jiao, C. Z. Sun and B. Tang, *Anal. Chem.*, 2017, **89**, 7210–7215.
- 47 M. Kumar, Y. N. Hong, D. C. Thorn, H. Ecroyd and J. A. Carver, *Anal. Chem.*, 2017, **89**, 9322–9329.
- 48 J. Wang, J. Mei, R. R. Hu, J. Z. Sun, A. J. Qin and B. Z. Tang, *J. Am. Chem. Soc.*, 2012, **134**, 9956–9966.
- 49 H. Q. Peng, X. Y. Zheng, T. Han, R. T. K. Kwok, J. W. Y. Lam, X. H. Huang and B. Z. Tang, *J. Am. Chem. Soc.*, 2017, **139**, 10150–10156.
- 50 X. F. Fang, Y. M. Zhang, K. W. Chang, Z. H. Liu, X. Su, H. B. Chen, S. X. A. Zhang, Y. F. Liu and C. F. Wu, *Chem. Mater.*, 2016, **28**, 6628–6636.



Facile synthesis and separation of E/Z isomerization of aromatic-substituted tetraphenylethylene for investigating their fluorescent properties via single crystal analysis.